# Recent Progress in Transmission Soft X-Ray Microscope

**K. Takemoto, T. Ohigashi[1], M. Kimura, H. Fujii[2], H. Aratame[2], Y. Ohashi[2], K. Nakanishi[3], H. Namba[2] and H. Kihara**

**Abstract**

An X-ray microscope beamline (BL-12) was installed in the SR center in 1996 and has been operated for 12 years. Using this system, unique biological samples were observed. Until now, several significant improvements were executed. A cryogenic object sample stage was developed and installed at BL-12. The set-up enables low-temperature imaging and applied in NIH 3T3 cell imaging. An auto-focusing imaging system was developed and installed at BL-12. The system can be controlled by a single finger and makes possible to perform the multi-wavelength imaging in a wide wavelength region from 1.73 to 4.73 nm. With the system, an edge absorption imaging can be easily applied to many elements.

*Department of Physics, Kansai Medical University, 18-89Uyama-higashi, Hirakata, Osaka, 573-1136, Japan*

*[1]Ritsumeikan University Research Organization of Science and Engineering, 1-1-1, Noji-Higashi, Kusatsu, Shiga, 525-8577, Japan*

*[2]Department of Physical Science, Ritsumeikan University, 1-1-1, Noji-Higashi Kusatsu, Shiga, 525-8577, Japan*

*[3]SR Center, Ritsumeikan University, 1-1-1, Noji-Higashi Kusatsu, Shiga, 525-8577, Japan*

## 1. Introduction

An X-ray microscope beamline (BL-12) was installed in 1996 and has been operated for 12 years. The present optical configuration of the X-ray microscope is the same with the previous one [1-2]. The optical system consists of two zone plates. In conjunction with a pinhole a condenser zone plate (CZP) acts as a dispersive and focusing element [3]. The CZP is a Göttingen KZP 7 type (diameter: 9 mm, outermost zone width: 53.7 nm, number of the zones: 41,890) [4]. The pinhole diameter is 15 μm. The objective zone plates (OZP) was fabricated at ZonePlates Ltd (diameter: 56 μm, outermost zone width: 45 nm, number of the zones: 311) [5]. The images are detected by a back-illuminated CCD (C4880-21-24WD, Hamamatsu K.K.). In ray tracing calculation, the wavelength resolution was estimated to be 300 at full-width at half maximum when a beam size was $0.28 \times 2.6\ \mu m^2$ ($2\sigma$) and distance between the source and the CZP of 7.1 m. Its resolution was estimated to be about 70 nm (20-80%) from the intensity gradient of the knife edge of the mesh [1, 2]. A computer controlled wavelength scanning system has been installed. The system covers 1.6 - 3.3 nm wavelength range [6, 7]. Energy calibration is performed by using nitrogen and oxygen absorption edges [8]. Multi-wavelength observation is currently highly demanded and is used for various experiments.

Until now, several significant improvements were executed. In 2004, development of a cryogenic sample observation project has started [9]. In BL-12, many of samples are biological and polymer specimens. Since there is serious radiation damage during observation of such biological and polymer specimens at room temperature, high resolution and high quality imaging is difficult. Basic considerations of image contrast indicate that doses of $10^6$ Gy are involved in 50 nm resolution imaging with soft X-rays [10]. These doses are sufficient to cause immediate changes in living cells. As a result, it produces noticeable mass loss and shrinkage in some specimens. It is well known that cooling biological specimens till cryogenic area can greatly reduce radiation damage. Cryo-X-ray microscopy experiment at 113 K have shown essentially no observable mass loss at the 50 nm spatial resolution level with radiation doses up to $10^{10}$ Gy [11]. Therefore cryo-X-ray microscopy experiments system is necessary to observe living cells. After cooling power test of the cooling equipment, the cryogenic sample chamber was introduced into the beamline and sample-cooling tests were executed.

In 2007, we started a new project to develop a full auto-focusing imaging system in BL-12. The full auto-focusing imaging system was designed. This system can be controlled by a single finger. It makes possible to perform the multi-wavelength imaging in a wide wavelength region from 1.73 to 4.73 nm (0.72 to 0.26 keV) which includes water windows region completely. The wavelength region also includes many X-ray absorption edges (Table. 1). With this system, an edge absorption imaging is more easily applied to many elements.

In this article, the results of cooling tests of the cryogenic sample chamber and the detailed description of the new projects are presented. Some recent imaging results are also presented.

Table 1 Enable observation elements and their X-ray absorption edges.

| No | Element | K-edge (eV) | L-edge (eV) | M-edge (eV) |
|---|---|---|---|---|
| 6 | C | 284.2 | | |
| 7 | N | 409.9 | | |
| 8 | O | 543.1 | | |
| 9 | F | 696.7 | | |
| 18 | Ar | | 248.4 | |
| 19 | K | | 294.6 | |
| 20 | Ca | | 346.2 | |
| 21 | Sc | | 398.7 | |
| 22 | Ti | | 453.8 | |
| 23 | V | | 512.1 | |
| 24 | Cr | | 574.1 | |
| 25 | Mn | | 638.7 | |

| No | Element | K-edge (eV) | L-edge (eV) | M-edge (eV) |
|---|---|---|---|---|
| 44 | Ru | | | 280 |
| 45 | Rh | | | 307.2 |
| 46 | Pd | | | 335.2 |
| 47 | Ag | | | 368 |
| 48 | Cd | | | 405.2 |
| 49 | In | | | 443.9 |
| 50 | Sn | | | 484.9 |
| 51 | Sb | | | 528.2 |
| 52 | Te | | | 573 |
| 53 | I | | | 620 |

**2. Cryogenic System and cooling power test**

The microscope is separated to two vacuum parts, the CZP chamber and the OZP chamber. The sample stage is placed between the CZP chamber and the OZP chamber under atmospheric pressure [1, 2]. A cryogenic sample chamber also has to work under atmospheric pressure.

Design concept of the cryogenic sample chamber is described as followings:

(1) The equipment is designed to maintain the cryo-condition for 100 minutes without frost forming.

(2) The equipment is able to adapt to X-ray microscope at BL-12.

(3) The equipment contains the sample holder which can be easily mounted.

In order to achieve these, a new cryogenic sample chamber was designed and produced [9, 12]. The cryo-system is based on the X-ray microscopy beamline at BESSY [4]. The cryogenic system consists of a liquid nitrogen (LN2) dewar and a sample stage. A metal tray is put at the bottom of the sample stage. The metal tray and the dewar are connected by a silicone tube with thermal insulation directly, and LN2 flows from the dewar to the metal tray. The flow rate is controlled by a temperature sensor plugged into the sample position. In order to avoid frost forming, the sample stage is enclosed with a cryo-house which consists of a thermal insulation block and stainless steel metal cover box. The cryo-house obtains two gates with airlock flanges for inserting two vacuum lines from the CZP chamber and the OZP chamber. Because inside of the cryo-house is filled with dried nitrogen gas produced by liquid nitrogen evaporation, it is expected that formation of frost can be prevented.

Cryogenic tests of the system were performed [13]. Under several preset temperatures between 100 K and 200 K, the cryogenic stabilities were sufficient. In order to examine frost-forming, the gate was opened and the sample stage was observed. Frost free was achieved for about 5 minutes.

In practical cryo-observation, a frozen specimen has to be mounted on the cooled sample stage rapidly because ice melts at room temperature. A new sample holder unit which consists of a sample holder and a handy bracket was designed and produced [13].

The Cryogenic chamber was installed at BL-12 beamline and cooling test was performed. Figure 1 shows the cryogenic system and result of cooling test in BL-12. LN2 dewar vessel is located about 20 cm higher than cryogenic sample chamber position. Preset temperature is 173 K. The system shows good low-temperature stability.

Figure 2 shows a comparison of the room- and low-temperature X-ray irradiation results as obtained for collodion films by optical microscopy in reflection. Their irradiated morphologies show distinct differences: in the case of the room-temperature (Fig. 2 (a)), a 60 μm broad annular feature can be observed within the damaged region. In contrast, the 273 K micrograph (Fig. 2 (b)) shows only a dark annular like feature bordering the damaged region. The damaged region is smaller than that of room-temperature micrograph (Fig. 2 (a)). In the case of the 233 K (Fig. 2 (c)), a small damaged region with a 30 μm dark annular feature can only be observed. It is evident that the cryogenic system provides a superior reduction of radiation damage.

Figure 3 shows a first image using the cryogenic system. In Fig. 3 a NIH3T3 cell is depicted which was fixed with 2.5 % glutaraldehyde in buffer and washed in distilled water. After air-dried, the cell was cooled on the cryogenic sample stage at 233 K. We can't observe new knowledge here as a result of cooling to low temperatures. In order to obtain a better image, a vibration instability problem that occurred on a LN2 flowing instrument is due to be improved.

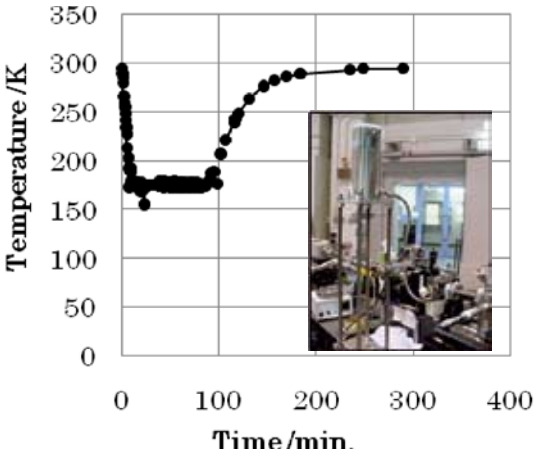


Figure 1 Cooling power and photograph of the cryogenic sample chamber at BL-12. Preset temperature was 173 K. After 100 min, the cooling was finished.

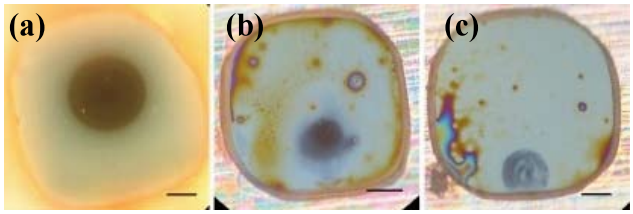


Figure 2 Demonstrate the damage caused by X-ray irradiation at various temperature in the collodion films (thickness 30 nm) with evaporated carbon films (thickness: 10 nm). Each preset temperature is (a) room temperature, (b) 273K, and (c) 233K. Wavelength was 2.3 nm and exposure time was 20 min. Scale bar: 20 μm.

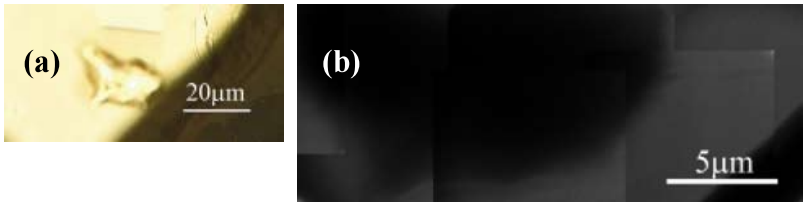


Figure 3 Light and X-ray microscopic images of a NIH3T3 cell. (a) Light microscopic image, (b) X-ray microscopic image at 233 K. Wavelength was 1.9 nm. Exposure time was 1 min.

**3. Improvement towards full auto-focusing imaging system**

The previous system was a half-automatic observation system [6, 7]. Because the CZP moves together with the CZP chamber by a stepping motor, usable wavelength range is restricted by a working stroke of a vacuum bellows which connected to the CZP chamber [1, 2].

In the new system, a CZP chamber was newly manufactured. A particular wavelength is selected by moving the CZP with a new stepping motor (ORIENTAL MOTOR Co., Ltd, Japan) along the optical axis of the synchrotron beam in it (see Figure 4). Figure 5 shows schematics and photographs of the mounting assembly for the CZP. The CZP is mounted on piezo positioner stages PP-30 for vacuum (MICOS, Germany). A central stop to prevent the first zero-order flux is also mounted on a 2-axis positioning stage with a tiny SQL Series SQUIGGLE motor SQ-100V for vacuum (New Scale Technologies, Inc, USA). The central stop stage is attached to a CZP holder plate and dependent moving to the CZP is possible. The new CZP chamber covers 1.73 - 4.73 nm wavelength range. Linear actuators are newly attached to the OZP and sample stages (Sigma, Japan). Technical data of the moving system have been collected in Table 2. As the results, every stage moving is computer-controlled by using a LabVIEW (National Instruments (NI)) system. With this system, user can control the system by a single finger and perform the multi-wavelength imaging in a wide wavelength

region from 1.73 to 4.73 nm. During the 2009 fiscal year, we look forward to observing bio-specimens with this new user-friendly X-ray microscope.

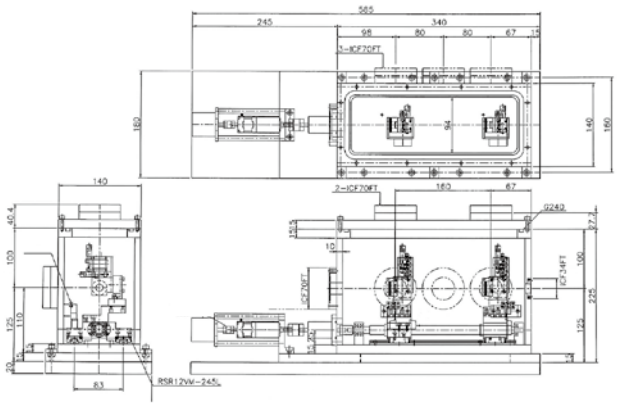

Figure 4 Schematic of new CZP chamber with the CZP stage.

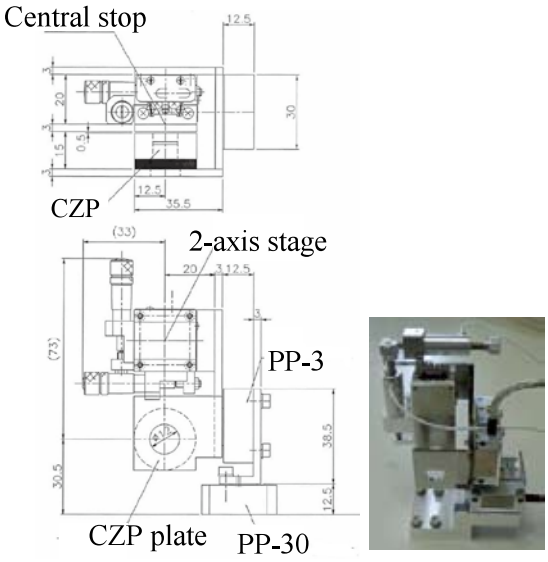


Figure 5 Schematic and photograph of mounting assembly for the CZP.

Table 2 Technical data of moving system of the new system.

| | CZP stage | | Central stage | OZP stage |
|---|---|---|---|---|
| | X (Optical axis) stage | Y, Z stage | Y, Z stage | X (Optical axis) stage<br>Y, Z stage |
| | Stepping motor (*ORIENTAL MOTOR Co., Ltd, Japan*) | Piezoelectric SQUIGGLE motor: SQ-100V (*New Scale Technologies, Inc, USA*) | Piezo positioner stages: PP-30 (*MICOS, Germany*) | 2-phase stepping motors:25ACTR-B0 (*Sigma, Japan*) |
| Travel | ±80 mm | ±5 mm | ±5 mm | ±12.5 mm |
| Resolution | 0.1 mm (full step) | 5 μm | 100 nm | 1 μm (full step) |
| Atmosphere | Atmospheric pressure | Vacuum ～$10^{-7}$ Torr | Vacuum $10^{-4}$ ～$10^{-9}$Torr | Atmospheric pressure |

## 4. Microscopic studies of biospecimens

### 4.1 Picophytoplankton

Lake Biwa is the largest lake in Japan. Recently, the chemical oxygen demand (COD) index of it is increasing in spite of a decrease in the values of biochemical oxygen demand

(BOD) index. This result suggests that an organic matter which is hard to decompose underwater has been increasing. Photosynthetic picoplankton which is the fraction of the plankton performing photosynthesis composed by cells between 0.2 and 2 μm is considered as an important source of the organic matter. Therefore, X-ray imaging of a microstructure of the picoplankton inhabiting Lake Biwa was performed. Figure 6 shows air-dried *Synechococcus* cells. Each cell has a dark sub-micron core. Because a *Synechococcus* cell is covered with agar layer, the low contrast region around the core can be interpreted as agar layer. Based on this interpretation, we aim at the identification of the amount in the existing layer of agar around *Synechococcus* cells.

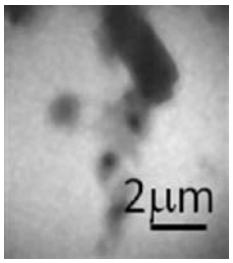


Figure 6 X-ray microscopic images of a *Synechococcus* cells taken at 2 nm. Exposure time was 5 min.

**4.2 Chromosome**

In order to clarify the process of condensation and distribution of a chromosome with nanometer-resolution, the process of cell division is observed by soft X-ray microscopy. We have previously reported that in prometaphase each chromosome was clearly visualized [14]. The thickness of a chromosome has not been uniform but varied from 150 nm to 750 nm.

In order to enhance electron density contrast for soft X-ray microscopy study, the staining of nuclei and chromosomes with the ammoniacal silver reaction was applied. Figure 7 (b) shows an X-ray microscopic photomontage image of mouse fibroblast cell line NIH3T3. About 6 photomicrographs are taken to form a photomontage with an area large enough for the study of chromosome.

Each chromosome is clearly visualized at high contrast. Thickness of a chromosome is uniform and the size is about 700 nm. However, fiber structure with a size of a few hundred nanometers is not observed. It is necessary to devise the dyeing of the chromosome.

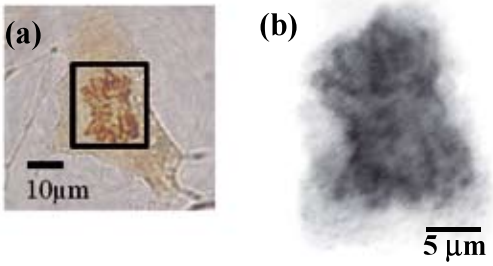


Figure 7 Light and X-ray microscopic images of a NIH3T3 cell at prometaphase in mitosis. (a) Light microscopic image. (b) X-ray microscopic photomontage image corresponding to the black square of (a) taken at 2 nm. This area corresponds with a photomontage of 6 micrographs Exposure time was about 30 min, 5 min/ micrograph × 6 micrographs.

### 4.3 *Deinococcus Radiodurans*

Soft X-ray microscope is expected to be one of the promising tools for observing living cells and tissues with nm order resolution. The most serious problem during the observation of living cells using soft X-ray microscopy is radiation damage of cellular components including DNA, protein and membrane lipid. In this study, *Deinococcus radiodurans* that possesses highly efficient mechanisms to protect oxidative damage was selected as the sample of X-ray microscopy observation.

Figure 8 shows an X-ray microscopic image of *D. radiodurans* cells. Observation wavelength was 2.3 nm and exposure time was 2 min. In Fig. 8, each cell with spherical-shaped structure had a dense body. Using a special cryogenic technique, we aim to produce the living cell observation with X-ray microscope.

.

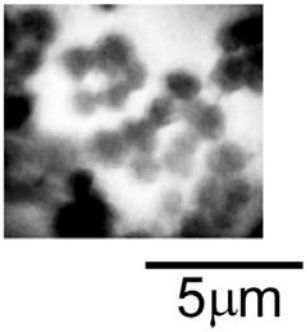


Figure 8 X-ray microscopic images of *Deinococcus radiodurans* cells. Observation wavelength was 2.3 nm and exposure time was 2 min.

## 5. Summary

An X-ray microscope beamline was installed in the SR center in 1996 and has been operated for 12 years. Using this system, many biological samples were observed and quite unique images were obtained. Until now, several significant improvements were executed. First cryo-X-ray microscopy experiment has been executed. An auto-focusing imaging system was designed and manufactured. The system can be controlled by a single finger and makes possible to perform the multi-wavelength imaging in a wide wavelength region from 1.73 to 4.73 nm. During the 2009 fiscal year, we look forward to observing bio-specimens with this new user-friendly X-ray microscope.

## Acknowledgements

This work was partly supported by Open Research Center Project for Private Universities matching fund subsidy from MEXT, 2007-2011. We are grateful to Ritsumeikan University SR Center staffs for their support. We thank Prof. Yamamoto at Nagahama Institute of Bio-Science and Technology for providing with us mouse fibroblast cell line NIH3T3. We also thank Dr. Ichise at Lake Biwa Environmental Research Institute for providing *Synechococcus* cells. We also thank Dr. Narumi and Dr. Satoh at Quantum Beam Science

Directorate, Japan Atomic Energy Agency for providing *Deinococcus Radiodurans*.

## References

[1] A. Hirai, K. Takemoto, K. Nishino, B. Niemann, M. Hettwer, D. Rudolph, E. Anderson, D. Attwood, D.P. Kern, Y. Nakayama and H. Kihara, *Jpn. J. Appl. Phys.* **38** (1999) 274-278.

[2] A. Hirai, K. Takemoto, K. Nishino, N. Watanabe, E. Anderson, D. Attwood, D. Kern, M. Hettwer, D. Rudolph, S. Aoki, Y. Nakayama and H. Kihara, *J. Synchrotron Rad* **5** (1998) 1102-1104.

[3] A. G. Michette, Optical systems for soft X rays, Plenum press, New York and London, 1986.

[4] G. Schmahl, D. Rudolph, B. Niemann, P. Guttmann, J. Thieme, G. Schneider, D. David, M. Diehl and T. Wilhein, *Optik* 93 (1995) 95-102.

[5] P. Charalambous, Proc. 8th Int. Conf. X-ray Microscopy IPAP Conf. Series **7** (2006) 127-129.

[6] K. Kimura, T. Takemoto and H. Kihara, Proc. 8th Int. Conf. X-ray Microscopy IPAP Conf. Series **7** (2006) 219-221.

[7] K. Takemoto, M. Kimura and H. Kihara**,** Memoirs of the SR center (Ritsumeikan Univ.) **6** (2004) 87-92.

[8] K. Takemoto, K Okuno, T. Fukui, Y. Yoshimura, T. Okamoto, H. Namba and H. Kihara**,** Memoirs of the SR center (Ritsumeikan Univ.) **8** (2006) 189-190.

[9] M. Kimura, K. Takemoto and H. Kihara**,** Memoirs of the SR center (Ritsumeikan Univ.) **7** (2005) 77-81.

[10] D. Sayre, J. Kirz, R. Feder, D. M. Kim and E. Spiller, *Ultramicroscopy* **2** (1977) 337-349.

[11] G. Schneider, *Ultramicroscopy* **75** (1998) 85-104.

[12] M. Kimura, K. Takemoto and H. Kihara**,** Memoirs of the SR center (Ritsumeikan Univ.) **9** (2007) 79-84.

[13] M. Kimura, K. Takemoto, Y. Ohashi, K. Nakanishi, H. Namba and H. Kihara, Memoirs of the SR center (Ritsumeikan Univ.) **10** (2008) 138-148.

[14] K. Takemoto, A. Yamamoto, I. Komura, K. Nakanishi, H. Namba and H. Kihara, Memoirs of the SR center (Ritsumeikan Univ.) **9** (2007) 85-89.